

Multi-responsive Chemosensors for Highly Sensitive and Selective Detection of Fe³⁺, Cu²⁺, Cr₂O₇²⁻ and Nitrobenzene based on Luminescent Lanthanide Metal–Organic Frameworks

Yi Du,^a Huayong Yang,^a Ruijuan Liu,^a Caiyun Shao,^a Lirong Yang^{a,*}

^aHenan Key Laboratory of Polyoxometalate Chemistry, College of Chemistry and Chemical Engineering, Henan University, Kaifeng, Henan 475004, P. R. China

Electronic Supplementary Information

Table S1 Selected bond lengths and bond angles for I–VI.

Table S2 Distances and angles of hydrogen bonds.

Table S3 Comparison of the corresponding lengths (Å, (average)) for I–VI.

Table S4 The ICP-AES data after 12 h of soaking in Fe³⁺ and Cu²⁺ ions.

Fig. S1 TGA curve of compound I–VI.

Fig. S2 PXRD patterns of compounds I–VI.

Fig. S3 The PXRD of I–V soaked into aqueous solutions with different pH values.

Fig. S4 (a) The excitation spectrum ($\lambda_{em} = 420$ nm) (black) and the emission spectra of H₄dpc, ($\lambda_{ex} = 339$ nm) (blue) of H₄dpc recorded at 298 K. (b) Luminescence decay of H₄dpc ligand.

Fig. S5 Luminescence decay of Eu-MOF.

Fig. S6 Solid-state luminescent spectrum of I–VI.

Fig. S7 The PXRD of Eu-MOF: as-synthesized and immersed in different cations solution.

Fig. S8 Comparison of the luminescence intensity (⁵D₀→⁷F₂) of Eu-MOF in sensing Fe³⁺ (a) and Cu²⁺ (c) with the interference of different cations solvents, red and blue bars represent the before and after the addition of Fe³⁺ (a) and Cu²⁺ (c), respectively. Quenching and recovery tests of Eu-MOF for Fe³⁺ (b) and Cu²⁺ (d) in DMF.

Fig. S9 The UV-vis adsorption spectra of various cations.

Fig. S10 (a) Comparison of the luminescence intensity (⁵D₀→⁷F₂) of Eu-MOF in sensing Cr₂O₇²⁻ with the interference of different anions solvents, red and blue bars represent the before and after the addition of Cr₂O₇²⁻. (b) quenching and recovery tests of Eu-MOF for Cr₂O₇²⁻ in DMF.

Fig. S11 The PXRD of Eu-MOF: as-synthesized and immersed in different anions solution.

Fig. S12 The UV-vis adsorption spectra of various anions.

Table S1 Selected bond lengths and bond angles for I–VI.

Bond lengths (Å)					
I					
La1-O7	2.405(4)	La1-O4	2.468(4)	La1-O9	2.550(5)
La1-O1	2.579(4)	La1-O2a	2.597(4)	La1-O2W	2.601(5)
La1-O2	2.620(4)	La1-O1W	2.633(5)	La1-O8	2.657(4)
II					
Ce1-O9	2.3724(19)	Ce1-O1	2.4358(19)	Ce1-O7	2.512(2)

Ce1-O4	2.5450(19)	Ce1-O1W	2.575(2)	Ce1-O3	2.5760(18)
Ce1-O2W	2.602(2)	Ce1-O3a	2.6043(18)	Ce1-O6	2.6322(19)
III					
Pr1-O8	2.3324(17)	Pr1-O2	2.3986(17)	Pr1-O6	2.4755(18)
Pr1-O5	2.5075(17)	Pr1-O4a	2.5317(17)	Pr1-O2W	2.5314(19)
Pr1-O1W	2.563(2)	Pr1-O4	2.5731(16)	Pr1-O7	2.6024(18)
IV					
Nd1-O5	2.3469(18)	Nd1-O9	2.4041(17)	Nd1-O1	2.4809(18)
Nd1-O6	2.5099(17)	Nd1-O1W	2.5321(19)	Nd1-O7a	2.5427(16)
Nd1-O2W	2.5648(19)	Nd1-O7	2.5888(17)	Nd1-O2	2.6109(17)
V					
Sm1-O5	2.316(2)	Sm1-O8	2.373(2)	Sm1-O1	2.450(2)
Sm1-O7	2.484(2)	Sm1-O2W	2.510(2)	Sm1-O6a	2.515(2)
Sm1-O1W	2.533(3)	Sm1-O6	2.586(2)	Sm1-O2	2.604(2)
VI					
Eu1-O1	2.293(6)	Eu1-O9	2.355(5)	Eu1-O5	2.437(6)
Eu1-O7	2.463(6)	Eu1-O2W	2.487(6)	Eu1-O6a	2.497(5)
Eu1-O1W	2.518(6)	Eu1-O6	2.576(6)	Eu1-O4	2.576(6)
Bond angle (°)					
I					
O7-La1-O4	82.38(15)	O7-La1-O9	129.57(15)	O4-La1-O9	87.98 (15)
O7-La1-O1	82.67 (14)	O4-La1-O1	140.30(15)	O9-La1-O1	129.07(15)
O7-La1-O2a	133.03(14)	O4-La1-O2a	135.95(13)	O9-La1-O2a	85.36(14)
O1-La1-O2a	50.76(13)	O7-La1-O2W	87.26(16)	O4-La1-O2W	75.75(15)
O9-La1-O2W	137.65(15)	O1-La1-O2W	66.98(15)	O2-La1-O2W	80.40(14)
O7-La1-O2	145.64(15)	O4-La1-O2	68.58(13)	O9-La1-O2	69.13(14)
O1-La1-O2	107.90(13)	O2-La1-O2a	68.38(14)	O2W-La1-O2a	68.54(14)
O7-La1-O1W	90.49(16)	O4-La1-O1W	145.50(15)	O9-La1-O1W	70.77(15)
O1-La1-O1W	70.98(15)	O2a-La1-O1W	70.78(14)	O2W-La1-O1W	137.85(15)
O2-La1-O1W	123.85(14)	O7-La1-O8	79.55(14)	O4-La1-O8a	72.90(15)
O9-La1-O8	50.45 (14)	O1-La1-O8	139.07(15)	O2-La1-O8	129.83(14)
O2W-La1-O8	147.26(15)	O2a-La1-O8	107.55(13)	O1W-La1-O8	72.61(14)
II					
O9-Ce1-O1	82.45(7)	O9-Ce1-O7	129.42(7)	O1-Ce1-O7	87.99(7)
O9-Ce1-O4	82.37(6)	O1-Ce1-O4	140.48(7)	O7-Ce1-O4	129.08(7)
O9-Ce1-O1W	86.57(8)	O1-Ce1-O1W	75.78(7)	O7-Ce1-O1W	138.49(7)
O4-Ce1-O1W	67.08(7)	O9-Ce1-O3	145.89(7)	O1-Ce1-O3	68.93(6)
O7-Ce1-O3	69.42(6)	O4-Ce1-O3	107.90(6)	O1W-Ce1-O3	69.10 (7)
O9-Ce1-O2W	90.14(8)	O1-Ce1-O2W	145.68(7)	O7-Ce1-O2W	71.06(7)
O4-Ce1-O2W	70.41(7)	O1W-Ce1-O2W	137.42(7)	O3-Ce1-O2W	70.20(7)
O9-Ce1-O3	132.82(6)	O1-Ce1-O3	136.48(6)	O7-Ce1-O3	85.22(6)
O4-Ce1-O3	50.92(6)	O1W-Ce1-O3	81.36(7)	O3-Ce1-O3a	68.45(7)
O2W-Ce1-O3	123.97(7)	O9-Ce1-O6	79.11(6)	O1-Ce1-O6	72.53(7)
O7-Ce1-O6	50.80(6)	O4-Ce1-O6	138.80(7)	O1W-Ce1-O6	146.58(7)

O3-Ce1-O6	129.92(6)	O2W-Ce1-O6	73.16(7)	O3-Ce1-O6	108.06(6)
III					
O8-Pr1-O2	82.69(6)	O8-Pr1-O6	129.64(6)	O2-Pr1-O6	87.85(6)
O8-Pr1-O5	81.75(6)	O2-Pr1-O5	140.53(6)	O6-Pr1-O5	129.31(7)
O8-Pr1-O4	132.44(6)	O2-Pr1-O4	136.70(5)	O6-Pr1-O4	85.23(6)
O5-Pr1-O4	51.17(5)	O8-Pr1-O2W	86.39(7)	O2-Pr1-O2W	75.91(6)
O6-Pr1-O2W	138.52(6)	O5-Pr1-O2W	67.11(6)	O4-Pr1-O2W	81.49(7)
O8-Pr1-O1W	89.75(7)	O2-Pr1-O1W	145.33(6)	O6-Pr1-O1W	71.19(6)
O5-Pr1-O1W	70.48(6)	O4-Pr1-O1W	70.37(6)	O2W-Pr1-O1W	137.53(6)
O8-Pr1-O4	146.06(6)	O2-Pr1-O4	69.09(6)	O6-Pr1-O4	69.42(6)
O5-Pr1-O4	108.08(5)	O4-Pr1-O4a	68.47(6)	O2W-Pr1-O4	69.14(6)
O1W-Pr1-O4	124.19(6)	O8-Pr1-O7	79.13(6)	O2-Pr1-O7	72.49(6)
O6-Pr1-O7	51.00(6)	O5-Pr1-O7	138.42(6)	O4-Pr1-O7	129.94(5)
O2W-Pr1-O7	146.58(6)	O1W-Pr1-O7	72.86(6)	O4-Pr1-O7a	108.39(5)
IV					
O5-Nd1-O9	82.83(6)	O5-Nd1-O1	129.75(6)	O9-Nd1-O1	87.92(7)
O5-Nd1-O6	81.45(6)	O9-Nd1-O6	140.44(6)	O1-Nd1-O6	129.38(6)
O5-Nd1-O1W	86.20(7)	O9-Nd1-O1W	75.73(6)	O1-Nd1-O1W	138.60(7)
O6-Nd1-O1W	67.20(6)	O5-Nd1-O7	132.54(6)	O9-Nd1-O7	136.58(6)
O1-Nd1-O7	84.91(6)	O6-Nd1-O7	51.59(5)	O1W-Nd1-O7	81.87(6)
O5-Nd1-O2W	89.35(7)	O9-Nd1-O2W	145.13(6)	O1-Nd1-O2W	71.26(7)
O6-Nd1-O2W	70.61(6)	O1W-Nd1-O2W	137.77(6)	O7-Nd1-O2W	70.68(6)
O5-Nd1-O7	146.24(6)	O9-Nd1-O7	69.22(6)	O1-Nd1-O7	69.43(6)
O6-Nd1-O7	108.07(5)	O1W-Nd1-O7	69.23(6)	O7-Nd1-O7a	68.17(6)
O2W-Nd1-O7	124.41(6)	O5-Nd1-O2	78.90(6)	O9-Nd1-O2	72.57(6)
O1-Nd1-O2	51.35(6)	O6-Nd1-O2	138.15(6)	O1W-Nd1-O2	146.32(6)
O7-Nd1-O2	129.91(6)	O2W-Nd1-O2	72.58(6)	O7-Nd1-O2	108.79(5)
V					
O5-Sm1-O8	82.82(8)	O5-Sm1-O1	130.17(8)	O8-Sm1-O1	87.31(8)
O5-Sm1-O7	80.83(8)	O8-Sm1-O7	140.85(8)	O1-Sm1-O7	129.78(8)
O5-Sm1-O2W	85.55(9)	O8-Sm1-O2W	75.72(8)	O1-Sm1-O2W	138.46(9)
O7-Sm1-O2W	67.75(8)	O5-Sm1-O6	132.60(7)	O8-Sm1-O6	136.88(7)
O1-Sm1-O6	84.64(8)	O7-Sm1-O6	52.25(7)	O2W-Sm1-O6	82.78(9)
O5-Sm1-O1W	89.04(9)	O8-Sm1-O1W	144.40(8)	O1-Sm1-O1W	71.77(9)
O7-Sm1-O1W	70.55(8)	O2W-Sm1-O1W	138.29(8)	O6-Sm1-O1W	70.93(9)
O5-Sm1-O6	146.15(8)	O8-Sm1-O6	69.62(7)	O1-Sm1-O6	69.34(8)
O7-Sm1-O6	108.23(7)	O2W-Sm1-O6	69.23(8)	O6-Sm1-O6a	67.90(8)
O1W-Sm1-O6	124.80(8)	O5-Sm1-O2	78.88(8)	O8-Sm1-O2	72.13(8)
O1-Sm1-O2	51.73(8)	O7-Sm1-O2	137.62(9)	O2W-Sm1-O2	145.66(9)
O6-Sm1-O2	129.76(7)	O1W-Sm1-O2	72.30(8)	O6-Sm1-O2	109.35(7)
VI					
O1-Eu1-O9	83.3(2)	O1-Eu1-O5	130.3(2)	O9-Eu1-O5	87.0(2)
O1-Eu1-O7	80.68(19)	O9-Eu1-O7	141.2(2)	O5-Eu1-O7	129.7(2)
O1-Eu1-O2W	85.4(2)	O9-Eu1-O2W	75.9(2)	O5-Eu1-O2W	138.5(3)

O7-Eu1-O2W	67.9(2)	O1-Eu1-O6	146.0(2)	O9-Eu1-O6	69.63(18)
O5-Eu1-O6	69.85(19)	O7-Eu1-O6	107.76(19)	O2W-Eu1-O6	68.79(19)
O1-Eu1-O1W	88.3(2)	O9-Eu1-O1W	143.5(2)	O5-Eu1-O1W	71.8(2)
O7-Eu1-O1W	70.9(2)	O2W-Eu1-O1W	138.8(2)	O6-Eu1-O1W	71.86(19)
O1-Eu1-O6	132.75(19)	O9-Eu1-O6	136.60(18)	O5-Eu1-O6	84.3(2)
O7-Eu1-O6	52.55(18)	O2W-Eu1-O6	83.1(2)	O6-Eu1-O6a	67.4(2)
O1W-Eu1-O6	125.72(19)	O1-Eu1-O4	79.03(19)	O9-Eu1-O4	71.85(19)
O5-Eu1-O4	51.76(19)	O7-Eu1-O4	137.7(2)	O2W-Eu1-O4	145.5(2)
O6-Eu1-O4	129.60(19)	O1W-Eu1-O4	71.69(19)	O6-Eu1-O4	129.60(19)

Table S2 Distances and angles of hydrogen bonds.

D	H	A	d(D-H)	d(H...A)	d(D...A)	∠(D-H...A)
C2	H2	O2	0.93	2.52	3.400(12)	158
C2	H2	O3	0.93	2.58	3.094(12)	115

Table S3 Comparison of the corresponding lengths (Å, (average)) for I-VI.

	I	II	III	IV	V	VI
Ln-OW	2.617	2.589	2.547	2.548	2.522	2.503
Ln-O _{carboxyl}	2.554	2.525	2.484	2.498	2.475	2.457
Ln...Ln	4.3159(20)	4.2833(5)	4.2204(13)	4.2500(6)	4.2322(5)	4.2202(10)

Remark: OW, oxygen atom of the coordinated water; O_{carboxyl}, oxygen atom of the carboxylic group, Ln-O_{carboxyl}, average length.

Table S4 The ICP-AES data after 12 h of soaking in Fe³⁺ and Cu²⁺ ions.

Ions	The initial concentration (mg/L)	Residual ion concentration in solution (mg/L)	Adsorption percentage (%)
Fe ³⁺	5.585	2.858	48.83
Cu ²⁺	6.355	6.250	16.52

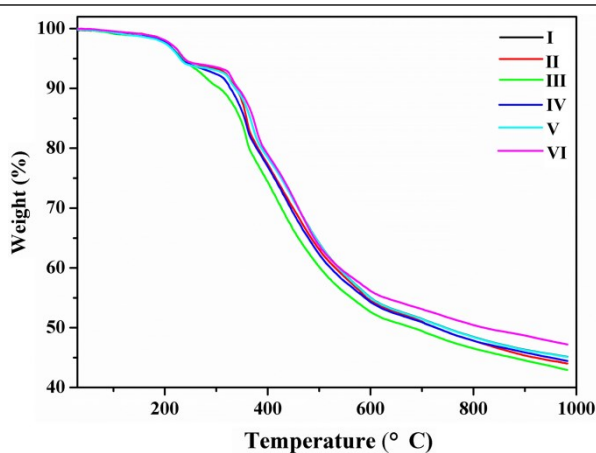


Fig. S1 TGA curve of compound I-VI.

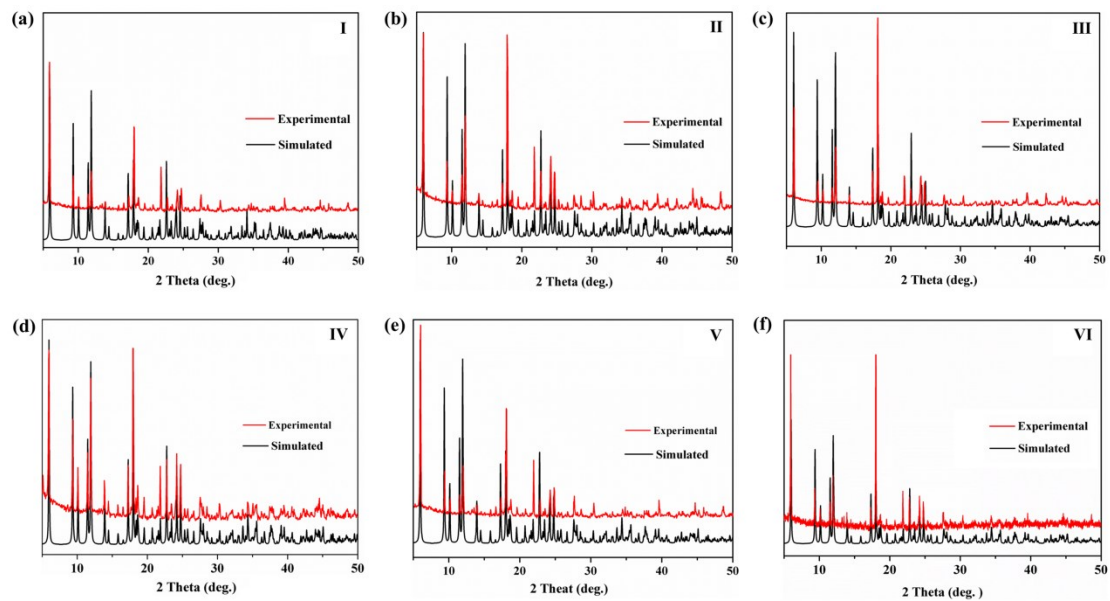


Fig. S2 PXRD patterns of compounds I-VI.

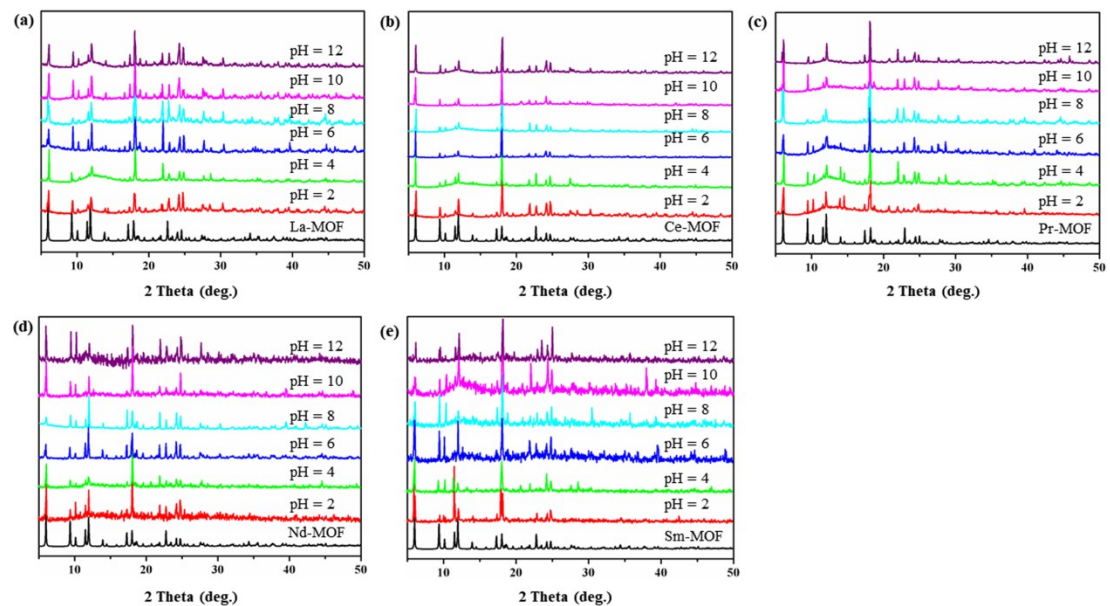


Fig. S3 The PXRD of I-V soaked into aqueous solutions with different pH values.

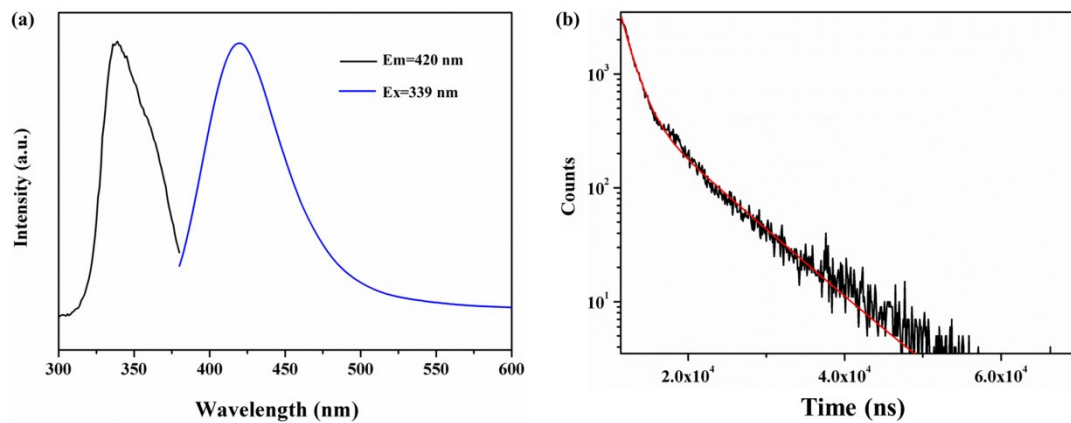


Fig. S4 (a) The excitation spectrum ($\lambda_{em} = 420$ nm) (black) and the emission spectra of H_4dpc , ($\lambda_{ex} = 339$ nm) (blue)

of H₄dpc recorded at 298 K. (b) Luminescence decay of H₄dpc ligand.

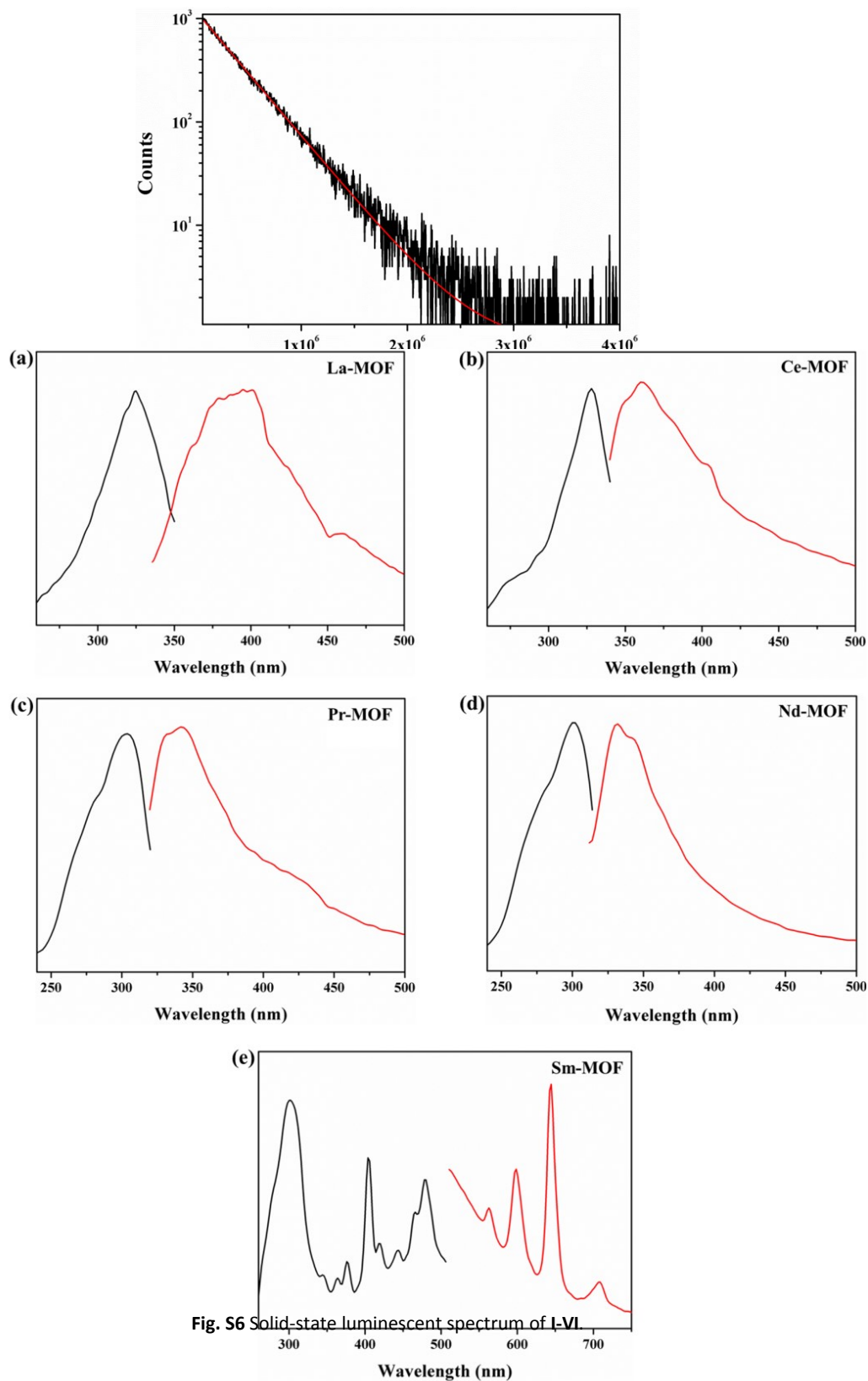


Fig. S6 Solid-state luminescent spectrum of I-VI

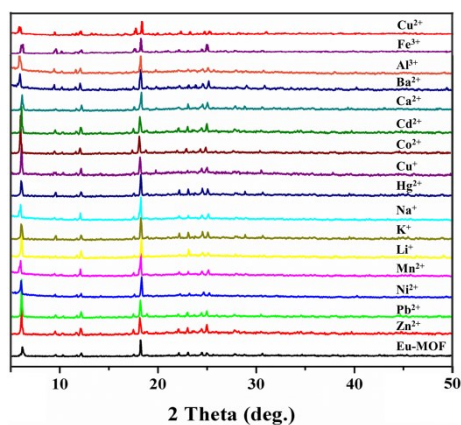


Fig. S7 The PXRD of Eu-MOF: as-synthesized and immersed in different cations solution.

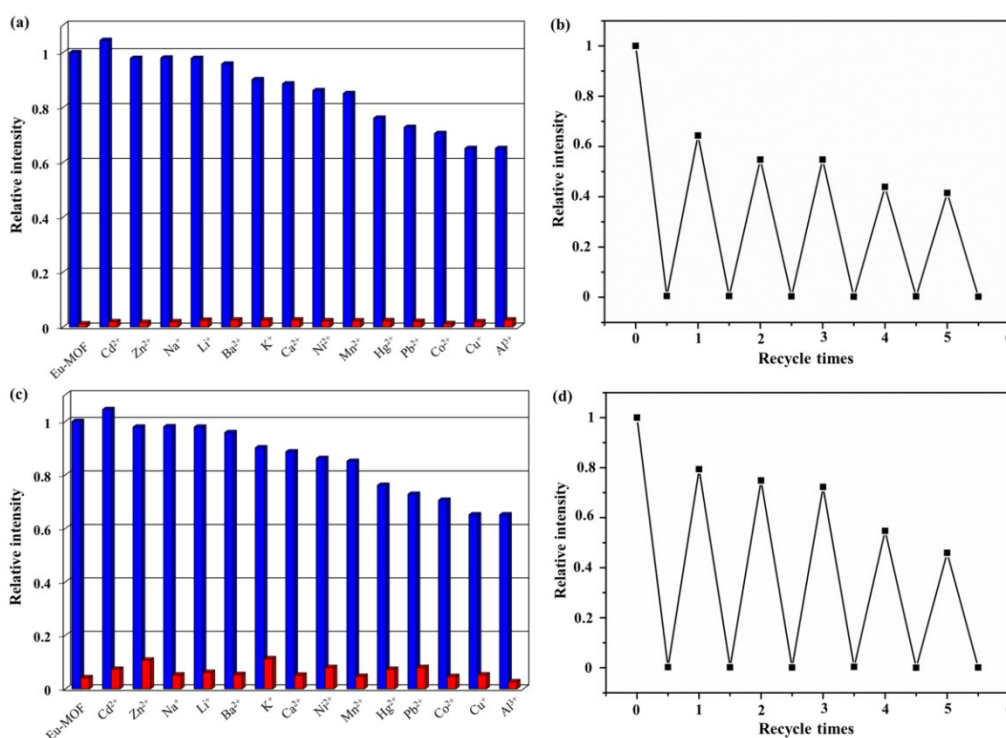


Fig. S8 Comparison of the luminescence intensity (${}^5D_0 \rightarrow {}^7F_2$) of Eu-MOF in sensing Fe³⁺ (a) and Cu²⁺ (c) with the interference of different cations solvents, red and blue bars represent the before and after the addition of Fe³⁺ (a) and Cu²⁺ (c), respectively. Quenching and recovery tests of Eu-MOF for Fe³⁺ (b) and Cu²⁺ (d) in DMF.

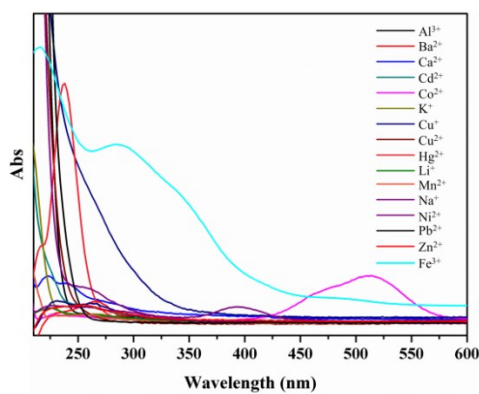


Fig. S9 The UV-vis adsorption spectra of various cations.

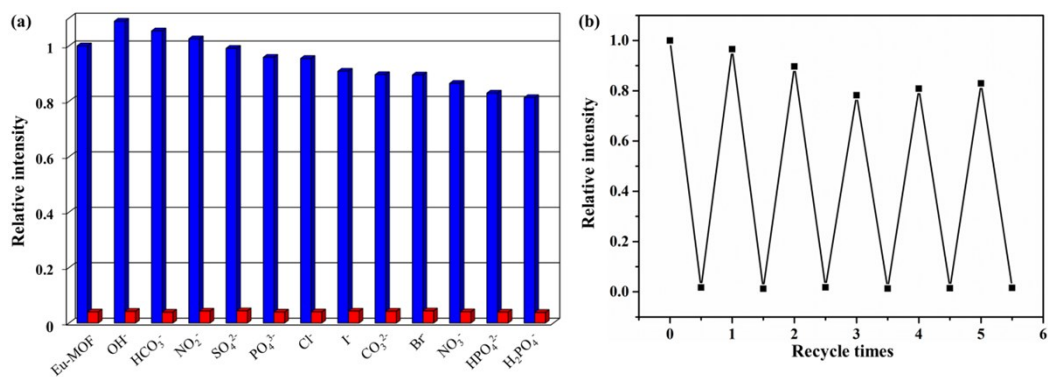


Fig. S10 (a) Comparison of the luminescence intensity ($^5\text{D}_0 \rightarrow ^7\text{F}_2$) of Eu-MOF in sensing $\text{Cr}_2\text{O}_7^{2-}$ with the interference of different anions solvents, red and blue bars represent the before and after the addition of $\text{Cr}_2\text{O}_7^{2-}$. (b) quenching and recovery tests of Eu-MOF for $\text{Cr}_2\text{O}_7^{2-}$ in DMF.

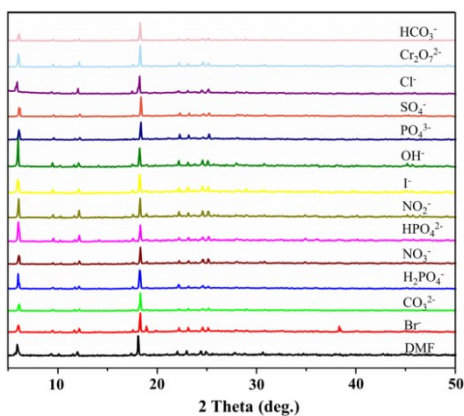


Fig. S11 The PXRD of Eu-MOF: as-synthesized and immersed in different anions solution.

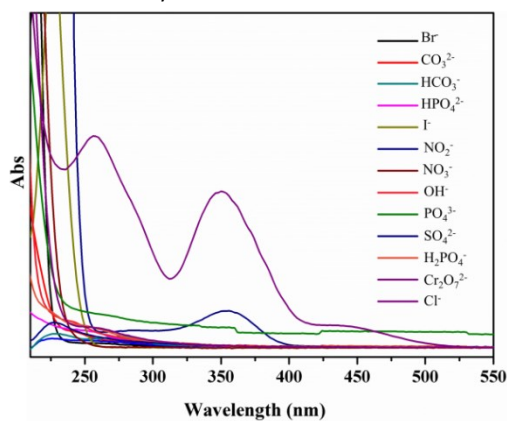


Fig. S12 The UV-vis adsorption spectra of various anions.